

# Shedding Light on (Anti-)nuclei Production with Pion-Nucleus Femtoscopy

Li-Yuan Zhang,<sup>1,2</sup> Che Ming Ko,<sup>3,\*</sup> Yu-Gang Ma,<sup>1,2,†</sup> Qi-Ye Shou,<sup>1,2,‡</sup> Kai-Jia Sun,<sup>1,2,§</sup> Rui Wang,<sup>4,¶</sup> and Song Zhang<sup>1,2,\*\*</sup>

<sup>1</sup>Key Laboratory of Nuclear Physics and Ion-beam Application (MOE),  
Institute of Modern Physics, Fudan University, Shanghai 200433, China

<sup>2</sup>Shanghai Research Center for Theoretical Nuclear Physics,  
NSFC and Fudan University, Shanghai 200438, China

<sup>3</sup>Cyclotron Institute and Department of Physics and Astronomy,  
Texas A&M University, College Station, Texas 77843, USA

<sup>4</sup>Istituto Nazionale di Fisica Nucleare (INFN), Sezione di Catania, I-95123 Catania, Italy

(Dated: November 18, 2025)

High-energy nuclear collisions provide a unique environment for synthesizing both nuclei and antinuclei (such as  $\bar{d}$  and  ${}^4\bar{\text{He}}$ ) at temperatures ( $k_B T \sim 100$  MeV) nearly two orders of magnitude above their binding energies of a few MeV. The underlying production mechanism, whether through statistical hadronization, nucleon coalescence, or dynamical regeneration and disintegration, remains unsettled. Here we address this question using a novel tool of pion-nucleus femtoscopy. By solving relativistic kinetic equations for pion-catalyzed reactions ( $\pi NN \leftrightarrow \pi d$ ) for deuteron production and including a  $70$  MeV/ $c^2$  downward shift of the in-medium  $\Delta(1232)$  mass, we successfully reproduce the resonance peaks observed by the ALICE Collaboration in both  $\pi^+ - p$  and  $\pi^+ - d$  femtoscopic correlation functions in high-multiplicity  $pp$  collisions at  $\sqrt{s} = 13$  TeV. We further find that the nucleon coalescence model reproduces only about half of the observed peak strength, while the statistical hadronization model predicts no resonance feature. These results provide compelling evidence that pion-catalyzed reactions play a dominant role in the production of light (anti-)nuclei in high-energy nuclear collisions and cosmic rays.

*Introduction.*— Loosely-bound light nuclei and antinuclei have been measured in high-energy nuclear collisions at Relativistic Heavy Ion Collider (RHIC) and the Large Hadron Collider (LHC) [1–4]. This phenomenon, known as ‘little-bang’ nucleosynthesis, has attracted renewed interest because of its relevance to matter–antimatter asymmetry tests [5], quark-gluon plasma (QGP) bulk properties [6], and indirect dark matter searches [7, 8]. Despite decades of study, the microscopic mechanism by which such fragile (anti-)nuclei form and survive the hot and dense hadronic environment remains unresolved [9–15].

Three major competing scenarios (see Figure 1) have been proposed, including statistical hadronization model (SHM) [16], nucleon coalescence at kinetic freeze-out [17, 18], and continuous disintegration and regeneration driven by pion-catalyzed reactions in the hadronic phase (e.g.  $\pi NN \leftrightarrow \pi d$ ,  $\pi Nd \leftrightarrow \pi {}^3\text{He}$ ) [19, 20]. Bulk observables such as yields,  $p_T$  spectra, and collective flow [21–25] alone cannot unambiguously distinguish these scenarios, as different models can reproduce similar integrated yields and flow patterns [19, 26].

In contrast, correlation femtoscopy [27, 28] or Hanbury-Brown and Twiss (HBT) interferometry [29–31] has evolved from its origins in astronomical intensity interferometry into a precision tool for probing the spatio-temporal structure of relativistic nuclear collisions, with sensitivity to length scales of order  $10^{-15}$  m and time scales of order  $10^{-23}$  s [32]. It has also become a powerful tool for studying the nature of strong interactions [33–36] and exotic hadrons [37]. Nontrivial femtoscopic correlations can arise from quantum statistics [38], final-state strong and Coulomb interactions [38, 39], or resonance decays [39]. Beyond its conventional applications to hadron–hadron pairs [40], femtoscopy has recently been extended to hadron–nucleus systems such as proton-deuteron

( $p - d$ ) [41, 42], kaon-deuteron ( $K - d$ ) [43], and deuteron-deuteron ( $d - d$ ) [44] pairs. For pion-catalyzed channels such as  $\pi^+ np \rightarrow \pi^+ d$ , the reaction rate peaks through formation of an intermediate  $\Delta(1232)$  resonance [20]. This would produce a characteristic resonant enhancement in the pion-deuteron ( $\pi - d$ ) correlation function, an effect not present in  $p - d$  or  $K - d$  correlations [41]. Such a resonance structure has recently been observed in both  $\pi^\pm - p$  and  $\pi^\pm - d$  correlations by the ALICE Collaboration [45, 46], though its microscopic origin remains to be clarified.

In the present study, we elucidate the ALICE measurements [45, 46] by solving relativistic kinetic equations for pion-catalyzed regeneration and breakup of (anti-)deuterons in  $pp$  collisions at  $\sqrt{s} = 13$  TeV and calculating pion-nucleus correlation functions. The resulting  $\pi^+ - p$  and  $\pi^+ - d$  correlation functions exhibit pronounced resonance peaks at  $k^* \simeq 0.2$  GeV/ $c$ , corresponding to  $\Delta$  excitation. From the comparison with ALICE data, we further reveal an in-medium  $\Delta$  mass reduction of roughly  $70$  MeV/ $c^2$ . Although the coalescence model reproduces similar qualitative trends, it explains only half of the observed peak magnitude, while the statistical hadronization model does not predict any resonance feature. These results demonstrate the unique discriminating power of pion–nucleus femtoscopy and identify pion-catalyzed reactions as the dominant mechanism for the production of light (anti-)nuclei in high-energy nuclear collisions.

*Theoretical framework.*— We employ a multi-phase transport (AMPT) model [47] to describe the evolution of the partonic phase created in  $pp$  collisions, with hadronization implemented via a quark coalescence mechanism. For the subsequent hadronic evolution and light (anti-)nuclei production, we include not only pion-catalyzed deuteron formation and dissociation but also other relevant scattering channels avail-

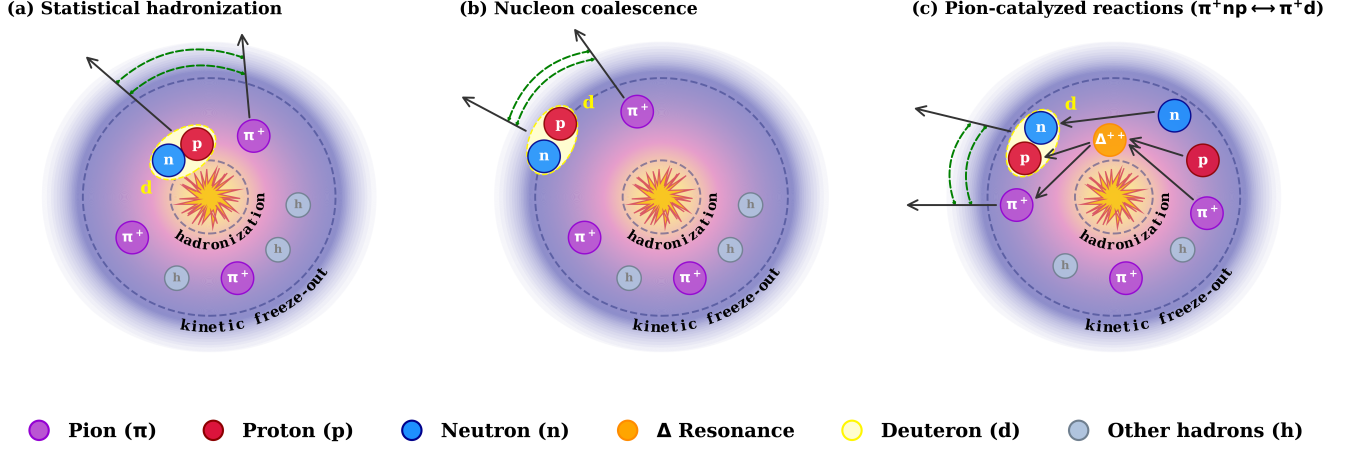


FIG. 1. Scenarios of deuteron production in high-energy nuclear collisions, including the statistical hadronization of QGP (a), the nucleon coalescence at the kinetic freeze-out (b), and the pion-catalyzed reactions (e.g.  $\pi^+np \leftrightarrow \pi^+d$ ) with the assistance of intermediate  $\Delta$  resonance during the hadronic matter expansion (c).

able in AMPT. These processes describe properly the dynamics of pions and nucleons that are essential for investigating light (anti-)nuclei production.

The effect of  $\pi^+d \leftrightarrow \pi^+np$  on deuteron production and dissociation in nuclear collisions can be described by the relativistic kinetic equation [20],

$$\frac{\partial f_d}{\partial t} + \frac{\mathbf{P}}{E_d} \cdot \frac{\partial f_d}{\partial \mathbf{R}} = -\mathcal{K}^> f_d + \mathcal{K}^<(1 + f_d), \quad (1)$$

where  $f_d(\mathbf{R}, \mathbf{P})$  denotes the phase space distribution of deuterons, and  $\mathcal{K}^>$  and  $\mathcal{K}^<$  denote respectively dissociation and regeneration rates with their expressions given in Ref. [20]. The effect of mean field is neglected due to the fact that the particle kinetic energy is much larger than the potential energy.

Equation (1) has been shown to successfully describe (anti-)deuteron production in Au+Au and Pb+Pb collisions [19, 20]. It was solved using a stochastic method with test particles [20]. In this method, the probability that the reaction  $\pi^+d \rightarrow \pi^+np$  occurs between a pion and a deuteron within the volume  $\Delta V$  during the time interval  $\Delta t$  under the impulse approximation (IA) is given by [20, 48–50]

$$P_{23}|_{\text{IA}} \approx F_d v_{\pi+p} \sigma_{\pi^+p \rightarrow \pi^+p} \frac{\Delta t}{N_{\text{test}} \Delta V} + (p \leftrightarrow n), \quad (2)$$

where  $v_{\pi+p}$  denotes the relative speed between the pion and the proton within the deuteron, and  $N_{\text{test}}$  refers to the number of test particles [51]. The pion-nucleon cross section is given by  $\sigma(E) = 2\pi g \tilde{\Gamma} \mathcal{A}(E) / q_0^2$  where  $\mathcal{A}(E)$  describes the spectral shape of the  $\Delta$  resonance using the Sill distribution [46, 52],

$$\mathcal{A}(E) = \frac{2E}{\pi} \frac{\sqrt{E^2 - E_{\text{th}}^2} \tilde{\Gamma}}{(E^2 - m_\Delta^2)^2 + (E^2 - E_{\text{th}}^2) \tilde{\Gamma}^2} \theta(E - E_{\text{th}}). \quad (3)$$

The rescaled width is defined as  $\tilde{\Gamma} = \Gamma_\Delta m_\Delta / \sqrt{m_\Delta^2 - E_{\text{th}}^2}$  with  $E_{\text{th}}$  being the threshold energy  $E_{\text{th}} = m_\pi + m_p$ . For all four

isospin states of  $\Delta$ , we take their width as  $\Gamma_\Delta = 0.117$  GeV and their mass as  $m_\Delta = 1.232$  (GeV/ $c^2$ ) +  $\delta m_\Delta$  where  $\delta m_\Delta$  is introduced as an in-medium mass shift and it vanishes in vacuum. For  $\pi^+ - p$  scattering, the statistical spin factor is  $g = 2$  and the reference momentum is taken as  $q_0 = 0.18$  GeV/ $c$  to reproduce the experimental data on  $\pi^+ - p$  cross section. Employing a constant value of  $F_d \approx 0.72$  yields an accurate description of the measured  $\pi + d$  dissociation cross sections [53] within the energy domain relevant to the present study.

A sufficiently large  $N_{\text{test}}$  is typically required for the convergence of numerical results. However, calculating femtoscopic correlation functions necessitates event-by-event simulations ( $N_{\text{test}} = 1$ ), as any  $N_{\text{test}} > 1$  artificially suppresses genuine particle correlations. To overcome this limitation, we replace the  $1/\Delta V$  factor in Eq. (2) with a Gaussian smearing function,  $S_{ij} = e^{-d_{ij}^2/(2l^2)} / (2\pi l^2)^{3/2}$ , where  $d_{ij}$  is the spatial distance between particles  $i$  and  $j$ , and  $l$  denotes the effective interaction range. This treatment mimics the scattering of two Gaussian wave packets [14]. With this modification, Eq. (2) is rewritten as

$$P_{23}|_{\text{IA}} \approx F_d v_{\pi+p} \sigma_{\pi^+p \rightarrow \pi^+p} S_{\pi^+p} \Delta t + (p \leftrightarrow n). \quad (4)$$

The choice of  $l$  does not affect the momentum correlations of the outgoing particles and it is set as  $l = 1.2$  fm in the following calculation.

Similarly, the probability for the reaction  $\pi^+np \rightarrow \pi^+d$  to take place in a time interval  $\Delta t$  is

$$P_{32}|_{\text{IA}} \approx \frac{3}{4} F_d v_{\pi+p} \sigma_{\pi^+p \rightarrow \pi^+p} S_{\pi^+p} W_d \Delta t + (p \leftrightarrow n), \quad (5)$$

where  $W_d$  stands for the deuteron Wigner function, characterizing the nonlocal features of the scattering as it depends simultaneously on the positions and momenta of the constituent nucleons inside the deuteron.

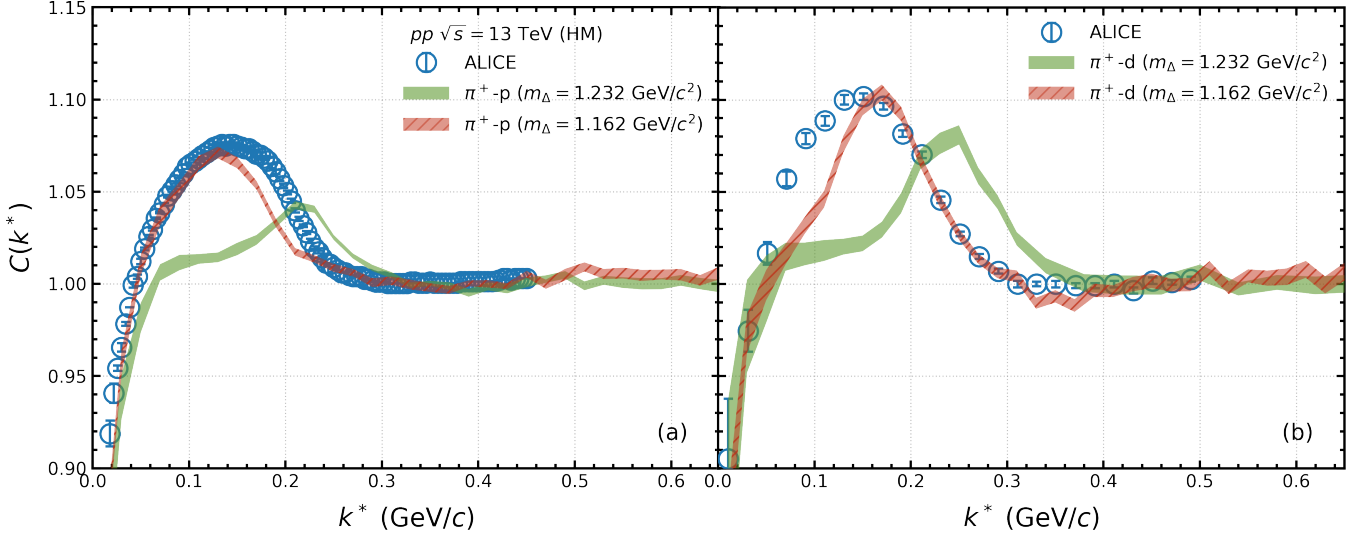


FIG. 2. Correlation function  $C(k^*)$  of  $\pi^+ - p$  (a) and  $\pi^+ - d$  (b) in high-multiplicity  $pp$  collisions at  $\sqrt{s} = 13$  TeV. Theoretical results with nominal and reduced  $\Delta$  masses are shown by green and red bands, respectively. Experimental data with combined statistical and systematic uncertainties taken from the ALICE Collaboration [45, 46] are denoted by filled symbols. Following the experimental kinematic cuts, particle rapidity is restricted to  $|\eta| \leq 0.8$ . The transverse momentum ( $p_T$ ) is required to be within the range  $0.14 < p_T < 4.0$  GeV/c for pions and  $0.5 < p_T < 2.4$  GeV/c for deuterons. For  $\pi^+ - p$  correlations, additional cut of pair transverse momentum, defined by  $m_T = \sqrt{(m_p + m_\pi)^2 + (\mathbf{k}_p + \mathbf{k}_\pi)^2}/2$ , of  $m_T \in [0.54, 0.75]$  GeV/c<sup>2</sup> is imposed [45].

With the obtained particle phase-space information at the kinetic freeze-out (defined as the phase-space positions at last collisions), the two-particle correlation function is then given by [28, 54]

$$C(\mathbf{k}^*) = \mathcal{N} \frac{\sum_{\text{pairs}}^{\text{same}} \delta(\mathbf{k}_{\text{pair}}^* - \mathbf{k}^*) |\Psi_{\mathbf{k}^*}(\mathbf{r}^*)|^2}{\sum_{\text{pairs}}^{\text{mixed}} \delta(\mathbf{k}_{\text{pair}}^* - \mathbf{k}^*)}, \quad (6)$$

where  $\mathbf{r}^* = \mathbf{r}_2 - \mathbf{r}_1$  is the relative spatial separation of the two particles after the earlier freeze-out particle is freely propagated to the time when the later one freezes out,  $\mathbf{k}^* = (\mathbf{k}_2^* - \mathbf{k}_1^*)/2$  is the reduced relative momentum in the pair rest frame (PRF), and  $\Psi_{\mathbf{k}^*}(\mathbf{r}^*)$  is the Bethe-Salpeter (BS) amplitude responsible for the final-state interactions (FSI). In the region of interest with small  $\mathbf{k}^*$ , the short-range particle interaction is dominated by the  $s$ -wave interaction, and the asymptotic solution of the wave function of the two charged particles is given in Refs. [32, 55]. The numerator represents the distribution of relative momenta between two particles emitted within the same collision event. Conversely, the denominator corresponds to the mixed-event distribution that serves as a reference that reflects the underlying phase space without the influence of FSI. Due to the small scattering parameters of the pion-nucleus pair, e.g., the scattering length of  $\pi^+ - d$  ( $p$ ) pair is about  $-0.037$  ( $-0.13$ ) fm [56, 57], the strong interaction contribution is thus small. The factor  $\mathcal{N}$  in Eq. (6) denotes the normalizing constant ensuring that  $C(k^*)$  is unity at large  $k^*$  where momentum correlation becomes negligible.

*Pion-nucleus femtoscopy in  $pp$  collisions at  $\sqrt{s} = 13$  TeV.*— We now compute the pion-nucleus femtosopic cor-

relation functions in high-multiplicity (HM) [58]  $pp$  collisions at  $\sqrt{s} = 13$  TeV using Eq. (6). Figure 2 displays the correlation functions  $C(k^*)$  for the pairs (a)  $\pi^+ - p$  and (b)  $\pi^+ - d$  from theoretical calculations as well as their comparison with experimental data from the ALICE Collaboration [45, 46], which are denoted by filled symbols together with their combined statistical and systematic uncertainties. Theoretical results using nominal  $\Delta$  mass  $m_\Delta = 1.232$  GeV/c<sup>2</sup> are represented by green bands (with charged particle multiplicity  $\langle dN_{\text{ch}}/d\eta \rangle \approx 26$ ) and display pronounced peaks at  $k^* \approx 0.22$  GeV/c. At the very low relative momentum  $k^* \leq 0.05$  GeV/c, correlation functions are suppressed by the repulsive Coulomb force between  $\pi^+ - p$  and  $\pi^+ - d$  pairs.

For the  $\pi^+ - p$  correlation, the peak originates from the decay  $\Delta^{++} \rightarrow \pi^+ + p$ . In the case of  $\pi^+ - d$  correlations, the peaks originate from forward pion-catalyzed reactions  $\pi NN \rightarrow \pi d$  whose rates are the largest in the excitation region of intermediate  $\Delta$  resonances [20]. Alternatively, in the  $\Delta$ -dominated region one may view these as sequential  $\Delta$ -assisted processes,  $\pi N \leftrightarrow \Delta$  and  $\Delta N \leftrightarrow \pi d$ . In both correlation functions, the ALICE data reveal pronounced peaks at a lower relative momentum of  $k^* \approx 0.15$  GeV/c. This downward shift was initially interpreted as a very low spectrum temperature  $k_B T \approx 20$ – $30$  MeV [45, 46], far below the typical kinetic freeze-out temperature usually higher than 100 MeV in  $pp$  collisions [59]. A more plausible explanation for the observed  $\Delta$  peak mass shift in  $pp$  collisions is its in-medium modification through interactions with the hot hadronic environment [60] or through partial restoration of chiral symmetry [61]. In particular, thermal QCD sum-rule calculations

predict a  $\Delta$  mass reduction of approximately 70 MeV at a temperature of  $T = 150$  MeV [62].

Similar shifts in the  $\Delta$  mass have been observed previously in minimum-bias  $pp$  and  $d$ +Au collisions at  $\sqrt{s_{NN}} = 200$  GeV [63], in Au+Au collisions at  $\sqrt{s_{NN}} = 2.4$  GeV [64], and in earlier fixed-target experiments [65, 66]. At low collision energies ( $\sqrt{s_{NN}} < 3$  GeV), these mass modifications were attributed to effects such as  $\Delta$  regeneration near the kinetic freeze-out stage [67, 68] and thermalization with cold nuclear matter [65, 69].

To phenomenologically account for this shift, we reduce the  $\Delta$  mass in our model from 1.232 to 1.162 GeV by setting  $\delta m_{\Delta} = -70$  MeV. The resulting  $\pi^+ - p$  correlation function, shown as the red band in Fig. 2 (a), now peaks at  $k^* \approx 0.15$  GeV/c, in much better agreement with the data. A similar mass shift is also observed in the  $\pi^+ - d$  correlation, where the peak moves from  $k^* \approx 0.22$  to 0.17 GeV/c. The model reproduces the experimental data well for  $k^* > 0.15$  GeV/c, but underestimates the correlation strength for lower  $k^*$  at 0.05 – 0.15 GeV/c. Further reducing the in-medium  $\Delta$  mass improves the description of the  $\pi^+ - d$  correlation but simultaneously worsens the agreement with the  $\pi^+ - p$  correlation. Improved agreements may be achieved in the future by extending the present kinetic approach to include off-shell effects of pions and nucleons within the  $S$ -matrix formalism [70] or the chiral effective field theory [71].

*Pion-nucleus femtoscopy in different production scenarios.*— We next investigate the pion-nucleus correlation functions within two alternative frameworks: the nucleon coalescence model [17] and the statistical hadronization model [16]. In the coalescence approach, deuterons form via  $n + p \rightarrow d$  at the kinetic freeze-out, and its number ( $N_d$ ) is given by [17]

$$N_d = \sum_{np} g_d W_d = \sum_{np} 6 \exp\left(-\frac{\rho^2}{\sigma_d^2} - \sigma_d^2 k_p^2\right), \quad (7)$$

where the summation is over all pairs of neutron and proton in each collision event,  $g_d = 3/4$  is the statistical factor for forming a deuteron of spin 1 from two spin 1/2 proton and neutron, the deuteron Wigner function  $W_d$  is taken to be Gaussian in spatial and momentum coordinates for simplicity. The Jacobi coordinates and momenta are defined by  $\rho = \mathbf{r}_2 - \mathbf{r}_1$ ,  $k_p = (\mathbf{k}_2 - \mathbf{k}_1)/2$  where  $\mathbf{r}_1$  and  $\mathbf{r}_2$  are the spatial coordinates of neutron, and proton, respectively, at an equal time in their rest frame, and they are determined by propagating the constituent nucleons of momenta  $\mathbf{k}_1$  and  $\mathbf{k}_2$  at earlier freeze-out times to the time of the later freeze-out one. The width parameter is taken as  $\sigma_d = \sqrt{8/3} r_d \approx 3.2$  fm to reproduce the deuteron size [72, 73].

The resulting  $\pi^+ - d$  correlation function from the coalescence model is shown by the purple band in Fig. 3. A residual correlation appears when one of the nucleons participating in  $n + p \rightarrow d$  originates from the  $\Delta$  decay, since the deuteron inherits the  $\pi - N$  correlation from its constituent. Conversely, if neither nucleon originates from a  $\Delta$ , no such correlation remains. Consequently, the coalescence-induced peak is significantly weaker than that generated by pion-catalyzed reac-

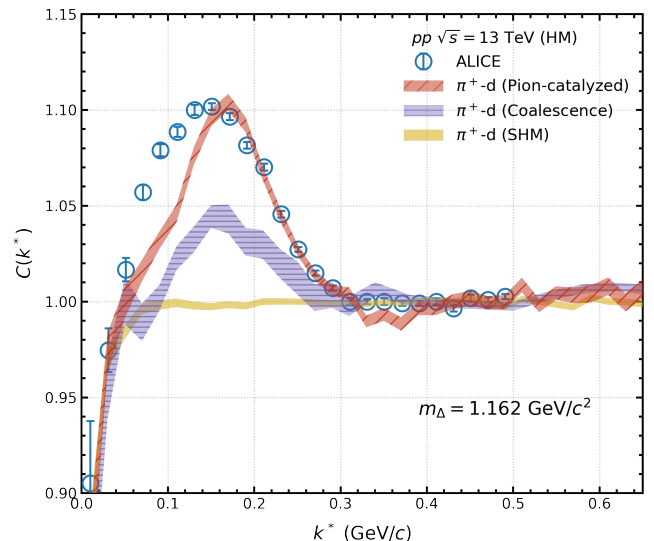


FIG. 3. Correlation function  $C(k^*)$  of  $\pi^+ - d$  in different production scenarios for  $pp$  collisions at  $\sqrt{s} = 13$  TeV. Experimental data shown as filled symbols are taken from the ALICE Collaboration [46], and theoretical predictions are represented by colored bands.

tions—less than half the strength observed in both the ALICE data and the pion-catalysis calculations (red band in Fig. 3).

In the statistical hadronization approach, pions and light nuclei are emitted independently from a thermalized expanding source, described here by a blast-wave parameterization using the parameters from Ref. [46]. After including the Coulomb interaction between the pion and deuteron, the calculated  $\pi^+ - d$  correlation function, shown by the yellow band in Fig. 3, exhibits the expected low- $k^*$  suppression due to repulsion but lacks any resonance-like structure associated with  $\Delta$  formation, consistent with results reported in Ref. [46].

The comparison in Fig. 3 demonstrates that the pion-catalyzed reaction framework provides the most accurate description of the ALICE data. The clearly distinct predictions of the three approaches highlight the strong discriminating power of pion-nucleus femtoscopy as a sensitive probe of the underlying dynamics of (anti-)nuclei production.

*Conclusion.*—In the present study, we have elucidated the production mechanism of light nuclei in high-energy nuclear collisions by employing the novel method of pion-nucleus femtoscopy, which enables clear differentiation among competing formation scenarios.

By solving relativistic kinetic equations for pion-catalyzed reactions ( $\pi NN \leftrightarrow \pi d$ ) on an event-by-event basis and including a 70 MeV/c<sup>2</sup> downward shift of the in-medium  $\Delta(1232)$  mass, we successfully reproduce the  $\Delta$  resonance peaks observed by the ALICE Collaboration in both pion-proton and pion-deuteron correlation functions in high-multiplicity  $pp$  collisions at  $\sqrt{s} = 13$  TeV. Although the nucleon coalescence model yields qualitatively similar structures, it underestimates the peak magnitude by roughly a factor of two, and the

statistical hadronization model predicts no resonance feature. Among the three considered scenarios, the pion-catalyzed reaction framework provides the most accurate and consistent description of the ALICE measurements (see Fig. 3), offering strong evidence that pion-catalyzed reactions dominate light (anti-)nuclei production at the LHC energies.

The present framework can be readily extended to larger collision systems such as  $p+Pb$ ,  $O+O$ ,  $Ru+Ru$ ,  $Zr+Zr$ ,  $Au+Au$ , and  $Pb+Pb$ , spanning beam energies from a few GeV to several TeV. Further exploration of femtosopic correlations involving heavier light nuclei, such as  $\pi$ - ${}^3\text{He}$ , pion-triton ( $\pi$ - ${}^3\text{H}$ ), pion-alpha ( $\pi$ - ${}^4\text{He}$ ), and pion-hypertriton ( $\pi$ - ${}^3_{\Lambda}\text{H}$ ) pairs, will provide deeper insight not only into the production dynamics of (anti-)(hyper-)nuclei in high-energy collisions and cosmic rays, but also into the formation mechanisms of more exotic states, such as  $X(3872)$  and  $T_{cc}^+$ , in extremely hot and dense environments.

*Acknowledgments.*— We thank Lie-Wen Chen, Mei-Yi Chen, Bhawani Singh, Laura Fabbietti, Yi-Heng Feng, Li-Sheng Geng, Feng-Kun Guo, Dimitar Mihaylov, Dai-Neng Liu, Pok Man Lo, Xiao-Feng Luo, Dong-Fang Wang, and Zhen Zhang for fruitful discussions. This work was supported in part by the National Key Research and Development Project of China under Grant No. 2024YFA1612500, the National Natural Science Foundation of China under Contracts No. 12422509, No. 12375121, No. 12025501, No. 12147101, No. 11891070, No. 124B2102, No. 12275054, No. 12061141008, Shanghai Pilot Program for Basic Research - Fudan University 21TQ1400100(22TQ006), the Guangdong Major Project of Basic and Applied Basic Research No. 2020B0301030008, and the STCSM under Grant No. 23590780100. The computations in this research were performed using the CFFF platform of Fudan University.

\* [ko@comp.tamu.edu](mailto:ko@comp.tamu.edu)

† Corresponding author: [mayugang@fudan.edu.cn](mailto:mayugang@fudan.edu.cn)

‡ [shouqiye@fudan.edu.cn](mailto:shouqiye@fudan.edu.cn)

§ Corresponding author: [kjsun@fudan.edu.cn](mailto:kjsun@fudan.edu.cn)

¶ [rui.wang@lns.infn.it](mailto:rui.wang@lns.infn.it)

\*\* Corresponding author: [song\\_zhang@fudan.edu.cn](mailto:song_zhang@fudan.edu.cn)

- [1] B. I. Abelev *et al.* (STAR), Observation of an Antimatter Hypernucleus, *Science* **328**, 58 (2010).
- [2] H. Agakishiev *et al.* (STAR), Observation of the antimatter helium-4 nucleus, *Nature* **473**, 353 (2011), [Erratum: *Nature* 475, 412 (2011)].
- [3] M. Abdulhamid *et al.* (STAR), Observation of the antimatter hypernucleus  ${}^4_{\Lambda}\bar{\text{H}}$ , *Nature* **632**, 1026 (2024).
- [4] S. Acharya *et al.* (ALICE), First Measurement of  $A = 4$  Hypernuclei and Antihypernuclei at the LHC, *Phys. Rev. Lett.* **134**, 162301 (2025).
- [5] ALICE Collaboration, Precision measurement of the mass difference between light nuclei and anti-nuclei, *Nature Phys.* **11**, 811 (2015).
- [6] D. Everett *et al.* (JETSCAPE), Role of bulk viscosity in deuteron production in ultrarelativistic nuclear collisions, *Phys. Rev. C* **106**, 064901 (2022).
- [7] P. von Doetinchem *et al.*, Cosmic-ray antinuclei as messengers of new physics: status and outlook for the new decade, *J. Cosmol. Astropart. Phys.* **08**, 035.
- [8] S. Acharya *et al.* (ALICE), Measurement of anti- ${}^3\text{He}$  nuclei absorption in matter and impact on their propagation in the Galaxy, *Nature Phys.* **19**, 61 (2023).
- [9] S. T. Butler and C. A. Pearson, Deuterons from High-Energy Proton Bombardment of Matter, *Phys. Rev.* **129**, 836 (1963).
- [10] J. I. Kapusta, Mechanisms for deuteron production in relativistic nuclear collisions, *Phys. Rev. C* **21**, 1301 (1980).
- [11] L. P. Csernai and J. I. Kapusta, Entropy and Cluster Production in Nuclear Collisions, *Phys. Rept.* **131**, 223 (1986).
- [12] P. Braun-Munzinger and B. Dönigus, Loosely-bound objects produced in nuclear collisions at the LHC, *Nucl. Phys. A* **987**, 144 (2019).
- [13] J. Chen, D. Keane, Y.-G. Ma, A. Tang, and Z. Xu, Antinuclei in Heavy-Ion Collisions, *Phys. Rept.* **760**, 1 (2018).
- [14] A. Ono, Dynamics of clusters and fragments in heavy-ion collisions, *Prog. Part. Nucl. Phys.* **105**, 139 (2019).
- [15] E. Braaten, K. Ingles, and J. Pickett, Explaining Snowball-in-Hell Phenomena in Heavy-Ion Collisions Using a Novel Thermodynamic Variable, *Phys. Rev. Lett.* **134**, 252301 (2025).
- [16] A. Andronic, P. Braun-Munzinger, K. Redlich, and J. Stachel, Decoding the phase structure of QCD via particle production at high energy, *Nature* **561**, 321 (2018).
- [17] R. Scheibl and U. Heinz, Coalescence and flow in ultrarelativistic heavy ion collisions, *Phys. Rev. C* **59**, 1585 (1999).
- [18] F. Bellini, K. Blum, A. P. Kalweit, and M. Puccio, Examination of coalescence as the origin of nuclei in hadronic collisions, *Phys. Rev. C* **103**, 014907 (2021).
- [19] D. Oliinychenko, L.-G. Pang, H. Elfner, and V. Koch (SMASH), Microscopic study of deuteron production in PbPb collisions at  $\sqrt{s} = 2.76\text{TeV}$  via hydrodynamics and a hadronic afterburner, *Phys. Rev. C* **99**, 044907 (2019).
- [20] K.-J. Sun, R. Wang, C. M. Ko, Y.-G. Ma, and C. Shen, Unveiling the dynamics of little-bang nucleosynthesis, *Nature Commun.* **15**, 1074 (2024).
- [21] S. S. Adler *et al.* (PHENIX), Deuteron and antideuteron production in Au + Au collisions at  $s(\text{NN})^{1/2} = 200\text{-GeV}$ , *Phys. Rev. Lett.* **94**, 122302 (2005).
- [22] S. Acharya *et al.* (ALICE), Production of light (anti)nuclei in pp collisions at  $\sqrt{s} = 13\text{ TeV}$ , *JHEP* **01**, 106.
- [23] S. Acharya *et al.* (ALICE), Enhanced Deuteron Coalescence Probability in Jets, *Phys. Rev. Lett.* **131**, 042301 (2023).
- [24] M. Abdulhamid *et al.* (STAR), Beam Energy Dependence of Triton Production and Yield Ratio ( $N_t \times N_p / N_d^2$ ) in Au+Au Collisions at RHIC, *Phys. Rev. Lett.* **130**, 202301 (2023).
- [25] B. Aboona *et al.* (STAR), Observation of Directed Flow of Hypernuclei  $\text{H}\Lambda 3$  and  $\text{H}\Lambda 4$  in  $s\text{NN}=3\text{ GeV}$  Au+Au Collisions at RHIC, *Phys. Rev. Lett.* **130**, 212301 (2023).
- [26] S. Acharya *et al.* (ALICE), Elliptic and triangular flow of (anti)deuterons in Pb-Pb collisions at  $\sqrt{s_{\text{NN}}} = 5.02\text{ TeV}$ , *Phys. Rev. C* **102**, 055203 (2020).
- [27] R. Lednický, Progress in correlation femtoscopy, in *32nd International Symposium on Multiparticle Dynamics* (2002) pp. 21–26, [arXiv:nucl-th/0212089](https://arxiv.org/abs/nucl-th/0212089).
- [28] M. A. Lisa, S. Pratt, R. Soltz, and U. Wiedemann, Femtoscopy in relativistic heavy ion collisions, *Ann. Rev. Nucl. Part. Sci.* **55**, 357 (2005).
- [29] R. Hanbury Brown and R. Q. Twiss, A Test of a new type of stellar interferometer on Sirius, *Nature* **178**, 1046 (1956).
- [30] G. Baym, The Physics of Hanbury Brown-Twiss intensity interferometry: From stars to nuclear collisions, *Acta Phys. Polon.*

- B **29**, 1839 (1998).
- [31] U. W. Heinz and B. V. Jacak, Two particle correlations in relativistic heavy ion collisions, *Ann. Rev. Nucl. Part. Sci.* **49**, 529 (1999).
- [32] R. Lednicky and V. L. Lyuboshits, Final State Interaction Effect on Pairing Correlations Between Particles with Small Relative Momenta, *Yad. Fiz.* **35**, 1316 (1981).
- [33] L. Adamczyk *et al.* (STAR), Measurement of Interaction between Antiprotons, *Nature* **527**, 345 (2015).
- [34] A. Collaboration *et al.* (ALICE), Unveiling the strong interaction among hadrons at the LHC, *Nature* **588**, 232 (2020), [Erratum: *Nature* 590, E13 (2021)].
- [35] S. Acharya *et al.* (ALICE), Scattering studies with low-energy kaon-proton femtoscopy in proton-proton collisions at the LHC, *Phys. Rev. Lett.* **124**, 092301 (2020).
- [36] D. Si *et al.*, Extracting Neutron-Neutron Interaction Strength and Spatiotemporal Dynamics of Neutron Emission from the Two-Particle Correlation Function, *Phys. Rev. Lett.* **134**, 222301 (2025).
- [37] M.-Z. Liu, Y.-W. Pan, Z.-W. Liu, T.-W. Wu, J.-X. Lu, and L.-S. Geng, Three ways to decipher the nature of exotic hadrons: Multiplets, three-body hadronic molecules, and correlation functions, *Phys. Rept.* **1108**, 1 (2025).
- [38] S. E. Koonin, Proton Pictures of High-Energy Nuclear Collisions, *Phys. Lett. B* **70**, 43 (1977).
- [39] U. A. Wiedemann and U. W. Heinz, Resonance contributions to HBT correlation radii, *Phys. Rev. C* **56**, 3265 (1997).
- [40] L. Fabbietti, V. Mantovani Sarti, and O. Vazquez Doce, Study of the Strong Interaction Among Hadrons with Correlations at the LHC, *Ann. Rev. Nucl. Part. Sci.* **71**, 377 (2021).
- [41] S. Acharya *et al.* (ALICE), Exploring the Strong Interaction of Three-Body Systems at the LHC, *Phys. Rev. X* **14**, 031051 (2024).
- [42] S. Mrowczynski, Two- versus three-body approach to femtoscopic hadron-deuteron correlations, *Phys. Lett. B* **864**, 139413 (2025).
- [43] O. Vázquez Doce, D. Mihaylov, and L. Fabbietti, Study of the deuterons emission time in pp collisions at the LHC via kaon-deuteron correlations, *Eur. Phys. J. A* **61**, 53 (2025).
- [44] S. Mrówczyński and P. Słoń, Deuteron-deuteron correlation function in nucleus-nucleus collisions, *Phys. Rev. C* **104**, 024909 (2021).
- [45] S. Acharya *et al.* (ALICE), Investigating the  $p$ - $\pi^\pm$  and  $p$ - $p$ - $\pi^\pm$  dynamics with femtoscopy in pp collisions at  $\sqrt{s} = 13$  TeV, *Eur. Phys. J. A* **61**, 194 (2025).
- [46] S. Acharya *et al.* (ALICE), Revealing the microscopic mechanism of deuteron formation at the LHC, (2025), [arXiv:2504.02393 \[nucl-ex\]](https://arxiv.org/abs/2504.02393).
- [47] Z.-W. Lin, C. M. Ko, B.-A. Li, B. Zhang, and S. Pal, A Multi-phase transport model for relativistic heavy ion collisions, *Phys. Rev. C* **72**, 064901 (2005).
- [48] P. Danielewicz and G. F. Bertsch, Production of deuterons and pions in a transport model of energetic heavy ion reactions, *Nucl. Phys. A* **533**, 712 (1991).
- [49] Z. Xu and C. Greiner, Thermalization of gluons in ultrarelativistic heavy ion collisions by including three-body interactions in a parton cascade, *Phys. Rev. C* **71**, 064901 (2005).
- [50] R. Wang, Z. Zhang, L.-W. Chen, and Y.-G. Ma, Nuclear Collective Dynamics in Transport Model With the Lattice Hamiltonian Method, *Front. in Phys.* **8**, 330 (2020).
- [51] C.-Y. Wong, Dynamics of nuclear fluid. VIII. Time-dependent Hartree-Fock approximation from a classical point of view, *Phys. Rev. C* **25**, 1460 (1982).
- [52] F. Giacosa, A. Okopińska, and V. Shastry, A simple alternative to the relativistic Breit-Wigner distribution, *Eur. Phys. J. A* **57**, 336 (2021).
- [53] P. A. Zyla *et al.* (Particle Data Group), Review of Particle Physics, *PTEP* **2020**, 083C01 (2020).
- [54] A. Kisiel, Non-identical particle femtoscopy at  $s(\text{NN})^{1/2} = 200$ -AGeV in hydrodynamics with statistical hadronization, *Phys. Rev. C* **81**, 064906 (2010).
- [55] R. Lednicky, Finite-size effects on two-particle production in continuous and discrete spectrum, *Phys. Part. Nucl.* **40**, 307 (2009).
- [56] T. E. O. Ericson, B. Loiseau, and A. W. Thomas, Determination of the pion nucleon coupling constant and scattering lengths, *Phys. Rev. C* **66**, 014005 (2002).
- [57] S. R. Beane, V. Bernard, E. Epelbaum, U.-G. Meissner, and D. R. Phillips, The S wave pion nucleon scattering lengths from pionic atoms using effective field theory, *Nucl. Phys. A* **720**, 399 (2003).
- [58] S. Acharya *et al.* (ALICE), Investigation of the  $p$ - $\Sigma^0$  interaction via femtoscopy in pp collisions, *Phys. Lett. B* **805**, 135419 (2020), [1910.14407](https://arxiv.org/abs/1910.14407).
- [59] S. Acharya *et al.* (ALICE), Multiplicity dependence of  $\pi$ , K, and p production in pp collisions at  $\sqrt{s} = 13$  TeV, *Eur. Phys. J. C* **80**, 693 (2020).
- [60] K. Azizi and G. Bozkır, Decuplet baryons in a hot medium, *Eur. Phys. J. C* **76**, 521 (2016).
- [61] J. M. Torres-Rincon, B. Sintès, and J. Aichelin, Flavor dependence of baryon melting temperature in effective models of QCD, *Phys. Rev. C* **91**, 065206 (2015).
- [62] Y.-J. Xu, Y.-L. Liu, and M.-Q. Huang, Temperature Dependence of Decuplet Baryon Masses from Thermal QCD Sum Rules, *Commun. Theor. Phys.* **63**, 209 (2015).
- [63] B. I. Abelev *et al.* (STAR), Hadronic resonance production in d+Au collisions at  $s(\text{NN})^{1/2} = 200$ -GeV at RHIC, *Phys. Rev. C* **78**, 044906 (2008).
- [64] J. Adamczewski-Musch *et al.*, Correlated pion-proton pair emission off hot and dense QCD matter, *Phys. Lett. B* **819**, 136421 (2021).
- [65] M. Eskef *et al.* (FOPI), Identification of baryon resonances in central heavy ion collisions at energies between 1-AGeV and 2-AGeV, *Eur. Phys. J. A* **3**, 335 (1998).
- [66] E. L. Hjort *et al.*, Delta resonance production in Ni-58 + Cu collisions at  $E = 1.97$ -A-GeV, *Phys. Rev. Lett.* **79**, 4345 (1997).
- [67] T. Reichert, P. Hillmann, A. Limphirat, C. Herold, and M. Bleicher, Delta mass shift as a thermometer of kinetic decoupling in Au + Au reactions at 1.23 AGeV, *J. Phys. G* **46**, 105107 (2019).
- [68] T. Reichert, P. Hillmann, and M. Bleicher,  $\Delta$  resonances in Ca+Ca, Ni+Ni and Au+Au reactions from 1 AGeV to 2 AGeV: Consistency between yields, mass shifts and decoupling temperatures, *Nucl. Phys. A* **1007**, 122058 (2021).
- [69] W. Weinhold, B. L. Friman, and W. Noerenberg, Thermodynamics of an interacting pi N system, *Acta Phys. Polon. B* **27**, 3249 (1996).
- [70] P. M. Lo, S-matrix formulation of thermodynamics with N-body scatterings, *Eur. Phys. J. C* **77**, 533 (2017).
- [71] V. Baru, J. Haidenbauer, C. Hanhart, A. E. Kudryavtsev, V. Lensky, and U.-G. Meissner, Role of the Delta(1232) in pion-deuteron scattering at threshold within chiral effective field theory, *Phys. Lett. B* **659**, 184 (2008).
- [72] G. Ropke, Light nuclei quasiparticle energy shift in hot and dense nuclear matter, *Phys. Rev. C* **79**, 014002 (2009).
- [73] K.-J. Sun, C. M. Ko, and B. Dönigus, Suppression of light nuclei production in collisions of small systems at the Large Hadron Collider, *Phys. Lett. B* **792**, 132 (2019).